Electrochemical Studies of Tantalum in Fluorochloroaluminate Melts at 200-450°C

Guang-Sen Chen,* Anna G. Edwards, and Gleb Mamantov*

Department of Chemistry, University of Tennessee, Knoxville, Tennessee 37996-1600

ABSTRACT

The electrochemistry of tantalum(V) species in sodium fluorochloroaluminate melts (10 mole percent NaF) has been investigated in the temperature range of 200 to 450°C using cyclic, normal pulse, and square wave voltammetries, exhaustive electrolysis, Raman and electronic spectroscopies, and x-ray diffraction methods. The electrochemical behavior of tantalum(V) is strongly dependent on temperature. Three main reduction waves are observed at a temperature of 300°C or higher. The first and second reduction waves merge into one wave at temperatures below 300°C The first reduction wave is associated with the reduction of tantalum(V) to tantalum(IV) species followed by a dimerization reaction which occurs very slowly at lower temperatures. The second reduction wave is believed to be the reduction of the tantalum(IV) dimer, Ta_2^{8+}, to a tantalum(III) species (probably Ta_2^{6+}). The tantalum(III) species decomposes resulting in the formation of the cluster, $Ta_6Cl_{12}^{3+}$. The last reduction wave is assigned to the reduction of the trivalent tantalum species to a divalent tantalum species, which is highly unstable and decomposes to form the tantalum cluster, $Ta_6Cl_{12}^{2+}$, and metallic tantalum. The clusters are slowly reduced to metallic tantalum.

The electrochemistry of tantalum is complicated by the existence of various compounds with different oxidation states, such as Ta^{5+}, Ta^{4+}, Ta^{3+}, Ta_6^{15+}, Ta_6^{14+}, Ta^{0} [1-4] in $AlCl_3$-NaCl melts.[5,6] McCarley *et al.*[2,3] reported that anhydrous low-valent tantalum halides can be synthesized by the reduction of tantalum(V) halides with aluminum metal at appropriate temperatures. The electrolytic reduction and oxidation of tantalum and other refractory metal species in molten halide salts,[7-13] organic solvents,[14] and room temperature melts[15] have received considerable attention, since these metals generally have very high melting points and high corrosion resistance.

We are interested in the electrochemistry and electroplating of refractory metals such as Nb, Ta, and W in alkali chloroaluminate and fluorochloroaluminate melts. von Barner *et al.*[5] have recently reported electrochemical and spectroscopic studies of tantalum species in $AlCl_3$-NaCl melts at 160-300°C. Tantalum(V) forms two different species, $TaCl_6^-$ and $TaCl_5$, in basic ($AlCl_3$/NaCl mole ratio <1) and moderately acidic $AlCl_3$-NaCl melts.[5,16] In addition, $TaOCl_4^-$ is formed in basic melts in the presence of small amounts of oxide ions.[5] The reduction of tantalum(V) in an acidic $AlCl_3$-NaCl [51-49 mole percent (m/o)] melt at 175°C is believed to follow the sequence, $Ta^{5+} + e^- = Ta^{4+}$, $2\ Ta^{4+} = Ta_2^{8+}$, $Ta_2^{8+} + 2e^- = Ta_2^{6+}$, $5\ Ta_2^{6+} = Ta_6^{14+} + 4\ Ta^{4+}$. This reduction leads to the formation of a tantalum cluster. Formation of metallic tantalum was not observed in the electrolysis at 175°C in the sodium chloroaluminate melts.

McCurry[17] investigated the electrochemical behavior of tantalum(V) in $AlCl_3$-NaCl melts saturated with NaCl, noted $AlCl_3$-$NaCl_{sat}$ melts, as a function of the oxide concentration in these melts. These studies resulted in a voltammetric method employing tantalum(V) as a probe to determine small amounts of dissolved oxide impurities in molten $AlCl_3$-$NaCl_{sat}$[6].

Several researchers[18-20] have described spectroscopic studies of the chlorobromoaluminate and chloroiodoaluminate melts. The various mixed ions $AlCl_xX_{4-x}^-$ (X = Br, I) were reported when $AlCl_4^-$ was mixed with $AlBr_4^-$ or AlI_4^-. Gilbert *et al.*[21] investigated the Raman spectroscopy of fluoride-containing chloroaluminate melts at 580-820°C. It was observed that fluoride replaced chloride progressively, depending on the molar ratio of NaF to $NaAlCl_4$, to form the species $AlCl_3F^-$, $AlCl_2F_2^-$, $AlClF_3^-$, and AlF_4^-.

Sodium fluorochloroaluminate melts are interesting media because the electrochemistry and spectroscopy of solutes can be examined over a large temperature range (from *ca.* 200 to 800°C or higher). The attack of Pyrex and quartz cells by these melts is much smaller than that by alkali fluoride melts.[21] The cathodic limit of the fluorochloroaluminate melts occurs at more negative potentials than that of sodium chloroaluminate melts at high temperatures (see below). There is sufficient molten phase in the $NaAlCl_4$-NaF (90-10 m/o) system at temperatures well below its liquidus temperature (395°C)[22] for the electrochemical studies. In this paper, we describe the electrochemical studies of tantalum(V) in oxide-free fluorochloroaluminate melts, $NaAlCl_4$-NaF (90-10 m/o), at 200-450°C.

Experimental

Aluminum chloride (Fluka, >99.0%) was purified by subliming it twice under vacuum in a sealed Pyrex tube.[5,6] Sodium chloride (Mallinckrodt, reagent grade) was dried under vacuum (<50 mTorr) at 450°C for at least 48 h. High purity sodium fluoride (AESAR, puratronic, 99.995%) and tantalum chloride (AESAR, puratronic, 99.99%) were used without further purification. Carbon tetrachloride (water, 0.001%) was purchased from Baxter Diagnostics, Incorporated.

$AlCl_3$-$NaCl_{sat}$ melts were prepared from purified aluminum chloride and vacuum-dried sodium chloride. The melts were saturated with NaCl at 175°C. Any remaining base metal impurities in the melts were removed by adding aluminum metal (AESAR, 99.999%) in the process of preparing the melts.

It is very important to eliminate small amounts of oxide species in the melts since the presence of the oxide species will complicate the electrochemical behavior of Ta, Nb, and W in these melts.[15,23-25] Recently, we reported the use of phosgene, $COCl_2$, to convert oxide species to the chloride species in basic alkali chloroaluminate melts.[24] Very recently, we have found that carbon tetrachloride can also remove oxides effectively. The treatment with CCl_4 has several advantages compared to the $COCl_2$-treatment including the ease of handling CCl_4. The details of this new method will be reported elsewhere.[26]

Sodium fluorochloroaluminate melts were prepared by mixing CCl_4-treated $AlCl_3$-$NaCl_{sat}$ salts with high purity

Downloaded on 2016-04-08 to IP 130.203.136.75 address. Redistribution subject to ECS terms of use (see ecsdl.org/site/terms_use) unless CC License in place (see abstract).

sodium fluoride in a suitable ratio, followed by premelting this mixture in a quartz tube.[21]

The electrochemical studies were performed in a Pyrex cell using a glassy carbon plate as a counterelectrode, a tungsten wire (0.5 mm in diam), platinum wire (0.5 mm in diam) or a glassy carbon rod as a working electrode, and a platinum wire directly immersed in the melts as a quasi-reference electrode. The reference electrode was a silver wire dipped in $AlCl_3$-$NaCl_{sat}$ melt containing 6.28 m/o AgCl and placed in a thin Pyrex bulb. The silver electrode was found to be very stable and reproducible even at high temperatures, while an aluminum reference electrode was not steady at high temperatures. The potential difference of the Ag/Ag(I) reference *vs.* Al in $AlCl_3$-$NaCl_{sat}$ at 175°C was found to be 1.090 ± 0.005 V. The platinum quasi-reference electrode was used as the reference electrode for the electrochemical measurements, since the resistance across the Pyrex membrane was very high. The potential differences between the platinum quasi-reference and the silver reference electrodes were measured using a high impedance multimeter (Keithley 173A) before taking any voltammograms. In this report, the potentials given are with respect to the silver reference electrode.

The exhaustive electrolyses were performed using a large surface area glassy carbon crucible as a working electrode. An aluminum coil sealed in a glass tube and separated by a beta-alumina diaphragm was used as a counterelectrode. We found that a beta-alumina diaphragm was suitable for the exhaustive electrolysis of a species with high vapor pressure since it is a good sodium ion conductor and is gas tight.

All handling of melts and solutes was done in a nitrogen filled dry box (moisture level <2 ppm). Cells and ampuls were torch sealed under vacuum (<50 mTorr).

An EG&G Princeton Applied Research (PAR) potentiostat/galvanostat (Model 273) connected to an IBM computer (PS/2 Model 70 386) utilizing the PAR M270 software package was used to obtain cyclic, normal pulse, and square wave voltammograms.

Raman spectroscopic measurements were performed as described previously.[21,27] A furnace of the proper optical design was constructed in-house and enabled the detection of Raman signals at 90° to the excitation beam. Fairly high power levels, typically 400 mW, were required because of losses at the windows of the furnace. The monochromator slits were set for a bandpass of 3 cm^{-1}.

Ultraviolet-visible absorption spectra were recorded at room temperature (25°C) in 10 mm path length quartz cells, using a Hewlett Packard 8452A diode array spectrophotometer or a Varian Cary 219 spectrophotometer.

The chemical analyses were performed by Schwarzkopf Microanalytical Laboratory, Incorporated.

Results

Characterization of the fluorochloroaluminate melts.— In this study, we focused our attention on the electrochemical behavior of tantalum(V) in sodium fluorochloroaluminate melt, $NaAlCl_4$-NaF (90-10 m/o). Sato *et al.*[22] investigated the phase properties of fluoride-containing sodium chloroaluminate systems using differential thermal analysis. Their results indicated that the system $NaAlCl_4$-NaF (90-10 m/o) exhibited two-phase transition temperatures, 395 and 152°C. Although some solid material precipitated from the solution at temperatures ≥200°C, the amount of liquid phase was sufficiently large to permit the use of this melt over a large temperature range.

Since it is important to know the composition of the liquid and solid phases of the fluorochloro melts at temperatures lower than the liquidus point, the liquid phase was analyzed by Raman spectroscopy and chemical analysis, and the solid phase was characterized by x-ray diffraction. Figure 1 shows the Raman spectra of the liquid phase of $NaAlCl_4$-NaF (89.86-10.14 m/o) melt at several temperatures. First, the sample was gradually heated to 550°C, at which temperature it was completely molten, and then the

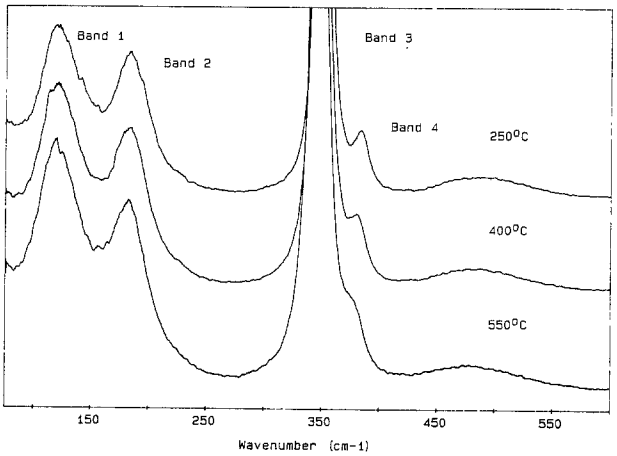

Fig. 1. Typical Raman spectra of the liquid phase of $NaAlCl_4$-NaF (89.86-10.14 m/o) melt at different temperatures (550, 400, and 250°C). Excitation wavelength, 488.0 nm; excitation power, 400 mW; bandpass, 3 cm^{-1}.

spectrum was acquired after 30 min of equilibration. Next, the temperature of the sample was gradually lowered and equilibrated at the lower level for at least 30 min prior to data acquisition. The frequencies of the observed bands are presented in Table I. The frequency of band 4 was obtained by deconvolution of band 3 and band 4 using a nonlinear least squares curve fitting technique. The deconvoluted bands were integrated to determine their areas. Bands 1, 2, and 3 were assigned to $AlCl_4^-$ species and band 4 to the fluorochloro species, $AlCl_3F^-$.[21] It is important to note that the band for the fluorochloro species, $AlCl_3F^-$, is observed at lower temperatures (even at 200°C). The ratio of $[AlCl_3F^-/AlCl_4^-]$ in the liquid phase was approximately constant in the temperature range studied since the area ratio of S_{Band4}/S_{Band3} was nearly independent of the temperature. It appeared that only a relatively small amount of the fluoride species precipitated at lower temperatures. This conclusion was supported by the chemical analysis of the liquid phases at 350 and 250°C, which contained 1.3 w/o and 0.86 w/o F, respectively, [the theoretical F content is 1.06 w/o in the $NaAlCl_4$-NaF (89.86-10.14 m/o) melt].

The results from Raman spectroscopy were in good agreement with the x-ray diffraction studies of the precipitate from the same melts at 250°C since the main compound in the precipitate was identified as NaCl. From these results, it is reasonable to conclude that the sodium chloroaluminate melts containing 10.14 m/o NaF, at temperatures below the liquidus point are fluorochloroaluminate melts saturated with NaCl.

The voltammetric characteristics of the fluorochloroaluminate melt differed from $AlCl_3$-$NaCl_{sat}$ melt at different temperatures. Typical cyclic voltammograms at a tungsten electrode at 450°C in these melts are shown in Fig. 2 and the cathodic limits are listed in Table II. The cathodic limit

Table I. Raman spectral data for the liquid phase of the $NaAlCl_4$-NaF (89.86-10.14 m/o) system.

t (°C)	Band 1 (cm^{-1})	Band 2 (cm^{-1})	Band 3 (cm^{-1})	Band 4 (cm^{-1})	S_{Band4} S_{Band3}
550	119.8	182.8	346.5	376.6	0.062
450	119.4	184.0	347.9	379.2	0.061
400	121.2	184.6	348.7	380.7	0.060
350	119.2	183.6	349.3	382.3	0.057
300	121.0	183.8	349.9	383.1	0.059
250	119.6	183.0	350.3	384.4	0.059
200	119.9	183.3	351.0	385.1	0.059

S_{Band4}/S_{Band3} is the area ratio of band 4 over band 3. The areas were obtained by integrating the deconvoluted band 3 and band 4, respectively.

Downloaded on 2016-04-08 to IP 130.203.136.75 address. Redistribution subject to ECS terms of use (see ecsdl.org/site/terms_use) unless CC License in place (see abstract).

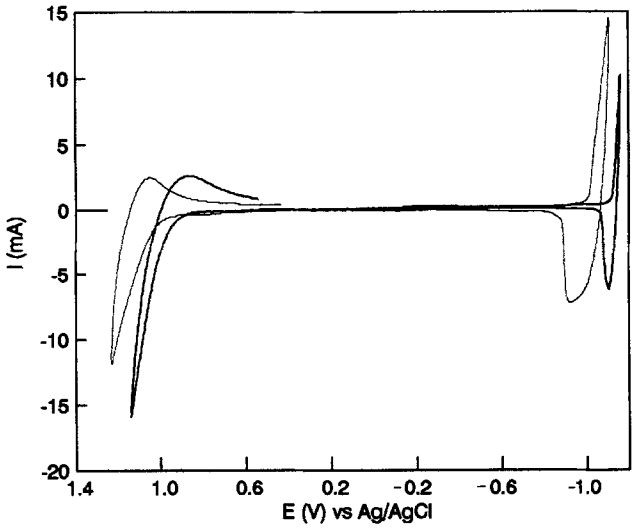

Fig. 2. Cyclic voltammograms at a tungsten electrode (0.175 cm²) in $AlCl_3$-$NaCl_{sat}$ melt (····) and $NaAlCl_4$-NaF (90-10 m/o) melt (———) at 0.1 V/s and 450°C.

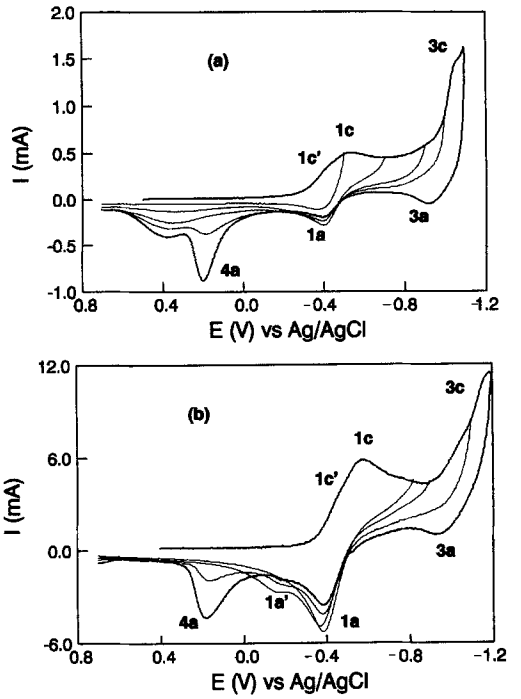

Fig. 3. Typical cyclic voltammograms of tantalum(V) at a tungsten electrode (0.175 cm²) at 250°C, (a) in the $AlCl_3$-$NaCl_{sat}$ melt with 5.65 × 10^{-3} mol/kg $TaCl_5$ at 0.1 V/s; (b) in the $NaAlCl_4$-NaF (90-10 m/o) melt with 37.6 × 10^{-3} mol/kg $TaCl_5$ at 0.5 V/s.

shifted to more positive values in both melts as the temperature was increased. The cathodic limit of the melt containing NaF was more negative at high temperatures than that of the melt without NaF added. This fact is important in studying the electrochemical behavior of Ta species, since the most negative reduction wave is very close to the cathodic limit (see below). An additional advantage of the fluorochloro melts over the saturated chloro melts is that the fluorochloro melts contain enough Cl^- ions to complex the Ta^{5+} species as $TaCl_6^-$ in the $TaCl_5$ concentration range studied (<0.3 mol/kg).[27]

The anodic limit in the fluorochloro melt occurred at less positive potentials than in the chloro melt at high temperatures. This is believed to be due to the higher free Cl^- activity in the former melt.

The electrochemical behavior of a glassy carbon electrode in this melt was identical to that of a tungsten electrode, while the behavior of a Pt electrode was complicated at high temperatures (>300°C) by the formation of Al-Pt alloys.

Cyclic voltammetry.—Several electrochemical techniques, including cyclic voltammetry, normal pulse voltammetry, square wave voltammetry, and exhaustive electrolysis were used to study the electrochemical behavior of tantalum species.

Figure 3 shows typical voltammograms of tantalum(V) obtained in the $AlCl_3$-$NaCl_{sat}$ melt (Fig. 3a) and in the fluorochloroaluminate melt, $NaAlCl_4$-NaF(90-10 m/o) (Fig. 3b) at 250°C. For convenience, the last cathodic wave is referred to as wave 3c since a new peak appears at high temperatures at a potential between the first and the second waves observed at low temperatures. It may be seen that the electrochemical behavior of the tantalum(V) species in the chloro melt is similar to that in the fluorochloro melt. It is noted that the peak potentials of waves 1c and 3c in the NaCl-saturated chloro melts are slightly more positive than the corresponding waves in the fluorochloro melts at the same $TaCl_5$ concentration. The cyclic voltammetric behavior seems to be more complicated in the chloro melts at high $TaCl_5$ concentrations (>*ca.* 50 m*M*) because $TaCl_5$ and $TaCl_6^-$ coexist in the chloro melt according to our recent Raman studies of the melt with a higher $TaCl_5$ concentration. These results indicate that as the concentration of $TaCl_5$ in the melt is increased the relative concentration of $TaCl_5$ to $TaCl_6^-$ increases as the concentration of Cl^- decreases due to complexation with $TaCl_5$. In the fluorochloro melts, only $TaCl_6^-$ was observed in the $TaCl_5$ concentration range studied, <0.3 mol/kg. Therefore, the electrochemistry of tantalum(V) species in the fluorochloro melt (10 m/o NaF) is the primary emphasis of this paper and the following discussion deals with studies in the fluorochloro melt unless otherwise specified.

Table II. Comparison of the cathodic limits of the $AlCl_3$-$NaCl_{sat}$ melt (E'_{0Cl}) and $NaAlCl_4$-NaF (90-10 m/o) melt (E'_{0F}).

t (°C)	E'_{0Cl} (V)	E'_{0F} (V)	E'_{0F}-E'_{0Cl}
200	−1.214	−1.171	0.043
250	−1.191	−1.196	−0.005
300	−1.130	−1.192	−0.062
350	−1.090	−1.188	−0.098
400	−1.069	−1.182	−0.113
450	−1.020	−1.130	−0.110

E'_0, the potentials at $i_c = 0$, were determined by extrapolating the Al(III) reduction current to zero. Scan rate 0.1 V/s.

Two main reduction waves were observed at lower temperatures. The first one (1c) was well defined while the second one (3c) was poorly defined. The anodic behavior was strongly dependent on the reversal potential. One oxidation wave (1a) was observed, which corresponded to wave 1c when the reversal potential was more positive than that of the onset of wave 3c. Two new anodic waves (3a and 4a) were observed when the potential was reversed at potentials corresponding to wave 3c. It is interesting to note that the small anodic wave (3a) was associated with wave 3c while the anodic wave 4a appeared at a much more positive potential than that of wave 1a. Wave 4a had the appearance of an anodic stripping wave of an insoluble species on the electrode surface.

The cyclic voltammetric behavior of the first redox couple (1c and 1a) of tantalum(V) at a tungsten electrode was found to be a function of the scan rate and temperature (200 and 250°C) as depicted in Fig. 4. As the scan rate was increased and the temperature was decreased, a cathodic shoulder (1c′) became more prominent. At lower scan rates (<0.5 V/s at 250°C), the shoulder almost disappeared. As shown in Table III, the cathodic peak potentials of wave 1c shifted to more negative values with an increase in the scan rate, while the half-peak potentials were essentially independent of the scan rate. It was noted that the ratio, $I_{pc}/v^{1/2}$, decreased as the scan rate increased.

Downloaded on 2016-04-08 to IP 130.203.136.75 address. Redistribution subject to ECS terms of use (see ecsdl.org/site/terms_use) unless CC License in place (see abstract).

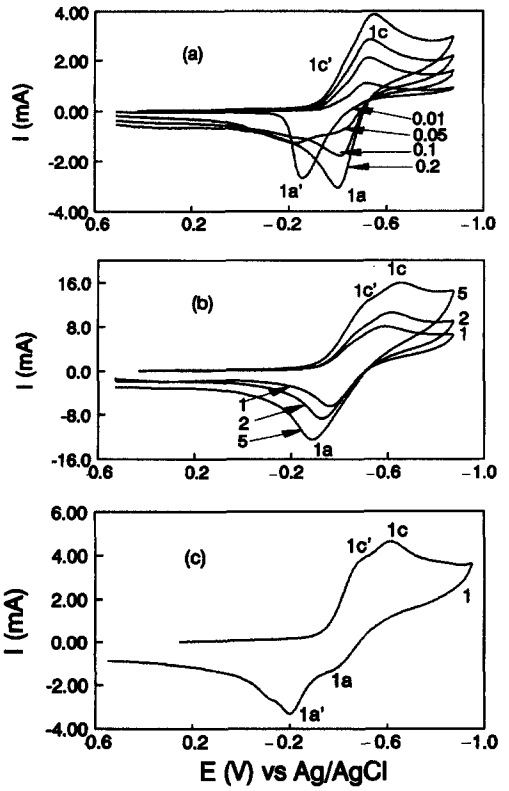

Fig. 4. The scan rate and temperature dependence of cyclic voltammograms of tantalum(V) species for the first redox couple in the fluorochloro melt with 34 × 10^{-3} mol/kg $TaCl_5$ (a) and (b) at 250°C, (c) at 200°C. A tungsten electrode (0.175 cm^2) was used. (a) 0.01, 0.05, 0.1, 0.2 V/s; (b) 1, 2, 5 V/s; (c) 1 V/s.

The anodic behavior (1a and 1a′) also changed with the scan rate. At high scan rates (>0.1 V/s), only one well-defined wave (1a) was observed while two anodic waves (1a and 1a′) appeared at 0.05 V/s. Wave 1a′ became the main anodic wave at 0.01 V/s and 250°C. At a relatively low temperature (200°C), the reaction associated with wave 1a′ dominated the anodic behavior even at 1 V/s (Fig. 4c).

The cathodic shoulder (1c′) was not observed at a higher $TaCl_5$ concentration (75.4 × 10^{-3} mol/kg). Both the peak potential and the half-peak potential of wave 1c tended to shift to more positive values as the $TaCl_5$ concentration was increased (Table IV). The slope of E_{pc} or $E_{(p/2)c}$ *vs.* ln (c) was determined to be in the range of 19 to 25 mV, which agreed with the expected value of 22.5 mV at 250°C for an EC reaction.[28,29]

The overall cyclic voltammograms of tantalum(V) at a tungsten electrode were influenced by the temperature. Typical cyclic voltammograms of tantalum(V) species at temperatures ranging from 300 to 450°C are shown in Fig. 5.

Table III. Cyclic voltammetric data for the first reduction wave of tantalum(V) (34 × 10^{-3} mol/kg) in the $NaAlCl_4$-NaF (90-10 m/o) melt.

v (V/s)	E_{pc}(V)	$E_{(p/2)c}$(V)	$I_{pc}/v^{1/2}$
0.01	−0.538	−0.453	10.43
0.05	−0.537	−0.446	8.96
0.10	−0.544	−0.441	8.54
0.20	−0.554	−0.441	8.11
0.50	−0.578	−0.440	7.83
1.00	−0.595	−0.437	7.45
2.00	−0.631	−0.447	6.86
5.00	−0.667	−0.449	6.71

I_{pv} in mA.
Tungsten electrode area: 0.175 cm^2.
Temperature: 250°C.

Table IV. The tantalum(V) concentration dependence of E_{pc} and $E_{(p/2)c}$ for the first reduction wave in the fluorochloro melt at 250°C and 0.1 V/s.

$TaCl_5$ (×10^{-3} mol/kg)	E_{pc}(V)	$E_{(p/2)c}$(V)
12.3	−0.551	−0.406[a]
34.0	−0.544	−0.441
37.6	−0.544	−0.445
79.5	−0.527	−0.432
138.8	−0.517	−0.427

[a] In the case of the lowest $TaCl_5$ concentration, wave 1c is significantly affected by the shoulder (1c′).

Three main reduction waves (1c, 2c, and 3c) were observed when the temperature was 350°C or higher. A small shoulder (3c′) also appeared. A new wave (2c) was observed at high temperatures (Fig. 5) and it became more pronounced as the temperature was increased. In other words, the first reduction wave observed at lower temperatures split into two waves at higher temperatures. The first wave (1c) seemed to change only slightly while the last two waves (2c and 3c) increased greatly as the temperature was increased.

The oxidation waves coresponding to waves 1c and 2c were ill-defined at higher temperatures in the overall cyclic voltammograms (Fig. 5) while waves 4a and 4a′ at positive potentials (between *ca.* 0 and *ca.* 0.4 V) were very pronounced. It was found that the anodic behavior was dependent on the reversal potential and the delay time (Fig. 6). When the cyclic voltammogram was reversed at a potential corresponding to wave 1c, only wave 1a was observed. This indicated that the reduced species corresponding to wave 1c was relatively stable at 450°C. A large anodic wave (4a) appeared if the reversal potential was extended to Wave 2c and a delay time was used (Fig. 6b). The corresponding anodic waves (1a and 2a) almost vanished. When

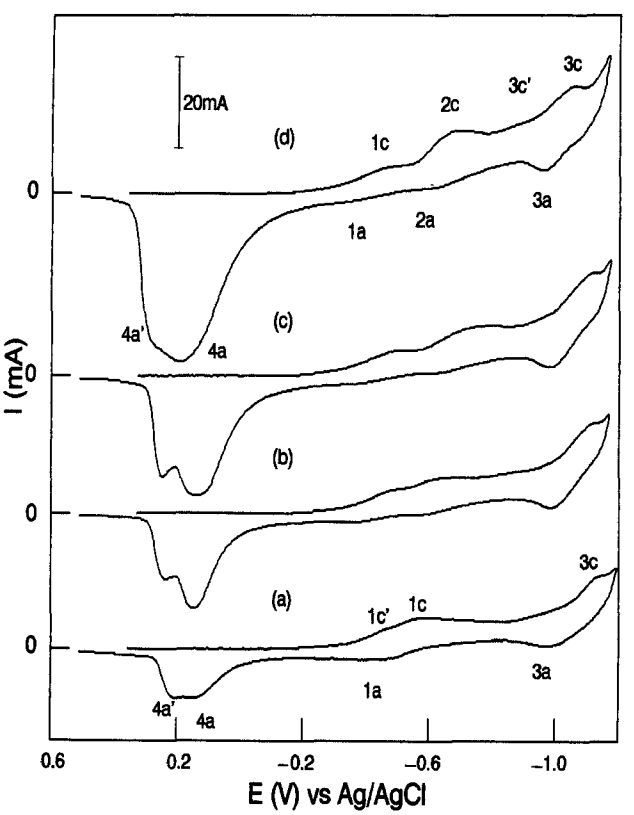

Fig. 5. The temperature dependence of the cyclic voltammograms of tantalum(V) at a tungsten electrode (0.175 cm^2) in the fluorochloro melt with 37.6 × 10^{-3} mol/kg $TaCl_5$ at (a) 300°C, (b) 350°C, (c) 400°C, and (d) 450°C. The scan rate was 0.5 V/s.

Downloaded on 2016-04-08 to IP 130.203.136.75 address. Redistribution subject to ECS terms of use (see ecsdl.org/site/terms_use) unless CC License in place (see abstract).

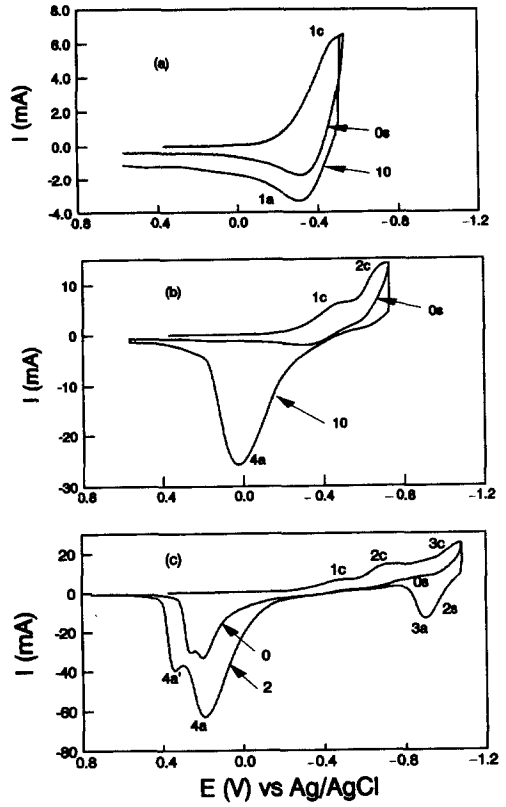

Fig. 6. Effects of the delay time at the reversal potential on the cyclic voltammograms of tantalum(V) (37.4×10^{-3} mol/kg) at a tungsten electrode (0.175 cm^2) at 450°C. The scan rate was 0.5 V/s. The delay times were (a) and (b): 0 s and 10 s; (c) 0 s and 2 s.

the reversal potential was extended to the third cathodic wave, the large anodic wave was composed of two waves (4a and 4a′) (Fig. 6c). A relatively small stripping wave (3a) was found in the cyclic voltammogram with a short delay time (2 s). During the electrolyses or electrodeposition using a small electrode, an insoluble black deposit was formed at potentials corresponding to the second or third wave. The black deposit was found to dissolve in ethanol forming yellow or green solutions. The spectra of these solutions are discussed below.

Normal pulse voltammetry.—Typical normal pulse voltammograms of Ta(V) at a tungsten electrode at different temperatures are shown in Fig. 7. It was evident that these voltammograms were strongly dependent upon temperature. At lower temperatures (<300°C), two main cathodic waves (waves 1 and 3) were observed. As the temperature was increased to 350°C or higher, another wave (wave 2) was observed; this wave became more pronounced at 400 and 450°C. The third wave (wave 3) grew significantly with temperature. This wave exhibited a maximum at a lower temperature (<350°C) when a short pulse width (0.1 s) was applied (Fig. 7). The maximum was diminished at a long pulse width (>0.5 s). The second wave was steeper than the first wave although the ratios of the second limiting current over the first limiting current were close to unity at 350 to 450°C (Table V).

According to Flanagan *et al.*,[30] no visible anomaly is present in the normal pulse voltammograms when only the reduced species are adsorbed. For a CE or EC process, plots of E *vs.* ln $[(I_d - I)/I]$ have the same slope as that for a simple redox reaction without a preceding or following chemical reaction.[31] Therefore, we can use the plots of E *vs.* ln $[(I_d - I)/I]$ to evaluate the n-values of waves 1 and 2 although these two waves may involve a following or a preceding chemical reaction.

The plots of E *vs.* ln $[(I_d - I)/I]$ for wave 1 at both 200-300°C and 400-450°C gave excellent linear curves. Typical results are summarized in Table V. It was found that the slopes of these plots for wave 1 agreed well with the theoretical values of (RT/nF) for $n = 1$ in a wide temperature range. A reasonable plot for wave 1 at 350°C could not be obtained since wave 2 is too close to wave 1. Linear relations of E *vs.* ln $[(I_d - I)/I]$ for wave 2 were also found at 400 to 450°C. An n-value of *ca.* 2 was found while the limiting current ratios of wave 2 over wave 1 were approximately 1 as mentioned above.

The plots of E *vs.* ln $[(I_d - I)/I]$ for wave 3 were not linear. The formation of a large amount of solid material on the electrode surface was observed at these potentials. The limiting current ratio of wave 3 over wave 1 was about three at 400-450°C, while it was approximately one at 350°C.

Square wave voltammetry.—Ramaley and Krause[32,33] developed the theory of square wave voltammetry for the hanging mercury drop electrode; however, the treatment was limited to small step heights (and consequently, slow scan rates). Osteryoung and coworkers[34-38] have made significant contributions to the theory of the square wave voltammetry including systems with coupled chemical reactions. Square wave voltammetry has previously been applied to studies of molten salt solutions.[39]

In the square wave voltammetry used in this work, the currents are sampled at the end of both the forward and reverse halves of the cycle. The net current is the difference of the forward current and the reverse current. For a simple reversible reaction, the net current-potential curve is bell shaped and symmetrical about the half-wave potential, and the peak height is proportional to concentration. The shape of the net current voltammogram is relatively insensitive to a variety of common complications in voltammetric experiments. The theoretical relationships for a reversible reaction are as follows for a pulse height of E_{sw} = 25 mV[35]

$$W_{1/2} = 3.91RT/nF \quad [1]$$

$$W_{1/2f} = 1.95RT/nF \quad [2]$$

where $W_{1/2}$ and $W_{1/2f}$ represent the total peak width and the front peak width at half height. These two equations may be used to estimate the n-values of reversible electron-transfer reactions preceded or followed by a chemical reaction since the peak width is not significantly dependent on

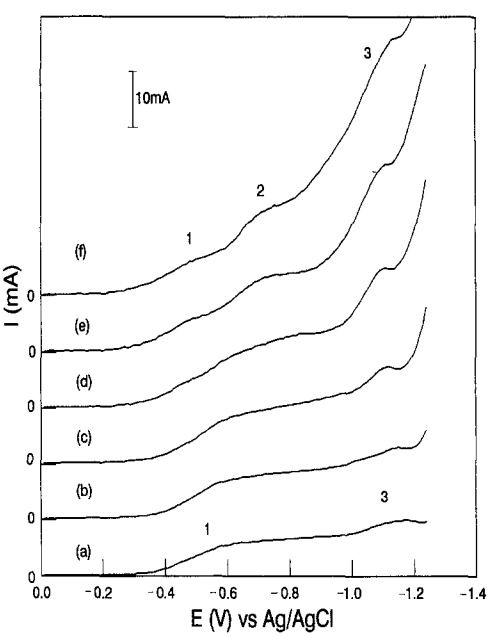

Fig. 7. Normal pulse voltammograms of tantalum(V) species in the $NaAlCl_4$-NaF (90-10 m/o) melt at (a) 200, (b) 250, (c) 300, (d) 350, (e) 400, and (f) 450°C. Tungsten electrode: 0.175 cm^2; $TaCl_5$ concentration: 37.6×10^{-3} mol/kg: pulse width: 0.1 s; step time: 0.5 s.

Downloaded on 2016-04-08 to IP 130.203.136.75 address. Redistribution subject to ECS terms of use (see ecsdl.org/site/terms_use) unless CC License in place (see abstract).

Table V. Normal pulse voltammetric data for the reduction of tantalum(V) (37.6×10^{-3} mol/kg) in the fluorochloro melt.

t (°C)	pw/s st/s	SL_1/mV n	$E_{(1/2)1}$ (V)	SL_2/mV n	$E_{(1/2)2}$ (V)	I_2/I_1	I_3/I_1
200	0.1	45.5	−0.481				0.40
	0.5	0.90					
200	1.0	40.6	−0.470				0.71
	5.0	1.01					
250	0.1	45.4	−0.488				0.53
	0.5	0.99					
250	1.0	41.9	−0.486				0.50
	5.0	1.07					
300	0.1	46.9	−0.471				0.79
	0.5	1.06					
300	1.0	48.4	−0.505				1.19
	5.0	1.02					
350	1.0	83.5	−0.565				0.82
	5.0	0.64					
400	0.1	55.8	−0.409	29.5	−0.639	1.11	2.9
	0.5	1.05		1.97			
400	1.0	58.3	−0.416	31.4	−0.640	1.30	3.17
	5.0	0.99		1.85			
450	0.1	59.2	−0.407	31.9	−0.649	1.30	3.33
	0.5	1.05		1.95			

pw: pulse width; st: step time; SL: the slope of E *vs.* $\ln[(I_d - I)/I]$; n: number of electrons.

the characteristics of the coupled chemical reactions and is close to the theoretical value for a simple reversible electron transfer reaction although the peak potential shifts negatively or positively.[37]

Figure 8A shows typical net-current square wave voltammograms of tantalum(V) at a tungsten electrode at temperatures from 200 to 450°C. These voltammograms were strongly dependent on temperature in agreement with the cyclic and normal pulse voltammograms discussed above. Only one well-defined wave (wave 1) appeared at 200°C. As the temperature was increased to 300°C or higher, a new wave (wave 2) appeared, and this wave became much better defined at temperatures higher than 350°C. This wave shifted to a more negative potential with temperature. Although wave 3 was ill-defined at temperatures lower than 300°C, it became well-defined at higher temperatures.

The peak heights and peak widths of wave 1 can be directly determined from the experimental results. For the case of wave 2, it is necessary to separate wave 2 from wave 1. Since the net-current voltammograms are bell-shaped and symmetric, the "back side" curve of wave 1 may be obtained by a symmetric extension. The "front side" of wave 2 is obtained by subtracting the back side of wave 1 from the experimental curve at the corresponding potentials. A typical result is shown in Fig. 8B. The peak height and width of wave 2 can be determined from the resulting wave.

The peak potentials and widths are presented in Table VI. It is obvious that wave 3 shifted to more positive potentials,

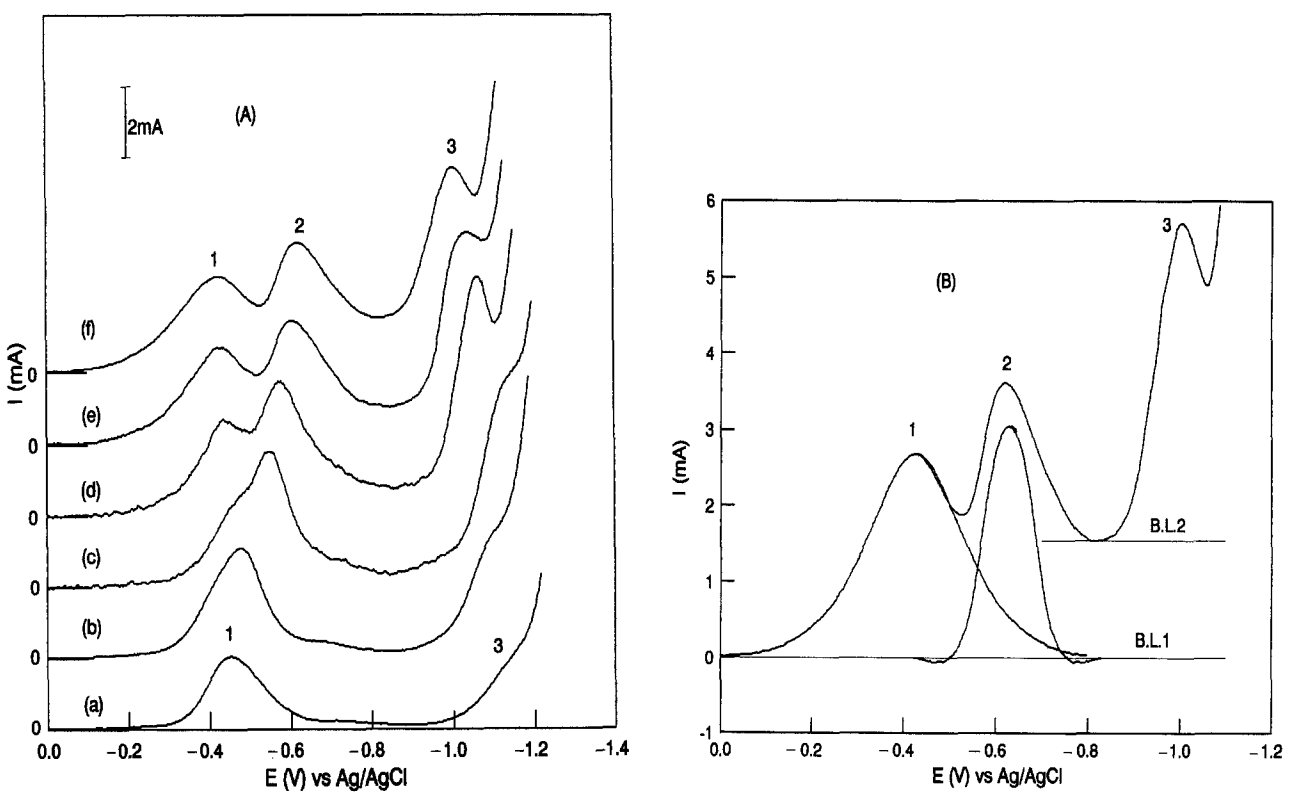

Fig. 8. (A) Net-current square wave voltammograms of tantalum(V) (37.6×10^{-3} mol/kg) in the $NaAlCl_4$-NaF(90-10 m/o) melt at (a) 200, (b) 250, (c) 300, (d) 350, (e) 400, and (f) 450°C. Tungsten electrode area: 0.175 cm^2; step potential: 2 mV; pulse amplitude (E_{sw}): 25 mV; frequency: 10 Hz. (B) Typical separation of wave 1 and wave 2. This voltammogram was obtained at 450°C and 100 Hz; step potential: 2 mV; E_{sw}: 25 mV; B. L. represents the base lines.

Downloaded on 2016-04-08 to IP 130.203.136.75 address. Redistribution subject to ECS terms of use (see ecsdl.org/site/terms_use) unless CC License in place (see abstract).

Table VI. Net-current square wave voltammetric data for tantalum(V) (37.6×10^{-3} mol/kg) in the fluorochloro melt.

t(°C)	Frq/Hz	$E_{(p)1}$(V)	$W_{(1/2f)1}$(mV)	n_1	$E_{(p)2}$(V)	$W_{(1/2f)2}$(mV)	n_2	I_{p2}/I_{p1}
200	100	−0.461	83.0	0.95				
200	10	−0.452	70.0	1.13				
250	100	−0.453	84.0	1.04				
250	10	−0.452	68.0	1.29				
300	100	−0.420	110	0.87				
350	100	−0.443	97.0	1.08	−0.555			
350	10	−0.434	72.0	1.45	−0.578	54.0	1.94	1.18
400	100	−0.446	110	1.03	−0.628	56.0	2.02	0.86
400	10	−0.422	90.0	1.25	−0.610	57.0	1.98	1.13
450	100	−0.425	120	1.01	−0.631	59.0	2.06	0.89
450	10	−0.426	120	1.01	−0.628	60.0	2.02	1.17

t(°C)	Frq./Hz		$E_{(p)3}$(V)	$W_{1/2f}$/(mV)	n_3	I_{p3}/I_{p1}
350	10	B.L.1	−1.058	58.0	1.80	2.47
		B.L.2	−1.058	51.0	2.05	2.17
400	100	B.L.1	−1.080	79.0	1.43	2.32
		B.L.2	−1.08	73.0	1.55	2.08
400	10	B.L.1	−1.040	75.0	1.51	2.19
		B.L.2	−1.038	65.0	1.74	1.85
450	100	B.L.1	−1.023	73.0	1.66	2.31
		B.L.2	−1.023	62.0	1.96	1.84
450	10	B.L.1	−1.002	81.0	1.50	2.13
		B.L.2	−1.002	63.0	1.93	1.63

E_{SW} = 25 mV; ΔE = 2 mV.
n-values were calculated from $W_{1/2f} = 1.95\ RT/nF$
$W_{1/2f}$: the front peak widths.
B. L.: Base line (see Fig. 8B).

while wave 2 moved in the opposite direction as the temperature was increased. The position of wave 1 was changed only slightly. The peak height ratios of wave 2 over wave 1, I_{p2}/I_{p1}, are close to one although they were slightly higher than one at a low frequency (10 Hz). The ratio of wave 3 to wave 1, I_{p3}/I_{p1}, was found to be between 1.6 and 2.5; it decreased slightly with an increase in temperature. The calculated n-values are given in Table VI. The n-value for wave 1 was close to unity although errors may be produced due to the shoulder observed in the cyclic voltammograms at a lower temperature (<300°C). The number of electrons involved in wave 2 was found to be two and that for wave 3 was between 1.5 and 2.05. These results are in good agreement with those obtained from normal pulse voltammograms (Table V).

Figure 9 shows typical square wave voltammograms for the forward and reverse currents. Three anodic waves were observed corresponding to the three cathodic reduction waves even at a higher temperature while these anodic waves were poorly defined in the cyclic voltammograms (Fig. 5 and 6). This may be due to the fact that the time between reduction and oxidation in square wave voltammetry was so short that only a small amount of the reduced species was consumed by the following chemical reactions. The chemical reaction following the electron charge transfer in wave 2 became faster at a higher temperature (450°C) as indicated by the fact that the anodic wave (wave 2a) almost disappeared at low frequencies (compare Fig. 9c and d).

Exhaustive and controlled-potential electrolyses of Ta(V).—It is clear that the electrochemistry of Ta(V) in these melts is complicated by coupled chemical reactions. Exhaustive coulometry provides additional information on the reduction process since the n-value for each reduction wave can be determined. The electrolyses were conducted both at a lower temperature (*ca.* 200°C) and a higher temperature (450°C) at different potentials. Typical results are summarized in Table VII.

For the first reduction wave at a lower temperature (see Fig. 3), the n-value was found to be approximately 2 when the electrolysis was performed at −0.75 V and 210°C. This result was quite surprising since the value of n = 1 was found from normal pulse and square wave voltammograms as mentioned above. The product dissolved in ethanol or distilled water to give an essentially colorless solution. Only a very weak band with an absorption maximum at *ca.* 330 nm was observed using UV-visible spectroscopy.

The electrolysis at −1.0 V and 205°C was carried out to investigate the last reduction wave (see Fig. 3). The voltammetric changes were monitored by interrupting the electrolysis and using a tungsten working electrode in this cell to record the voltammograms [cyclic voltammograms (CV) and square wave voltammograms (SWV)]. The cyclic voltammograms before the exhaustive electrolysis were identical to those shown in Fig. 3b. The electrolysis current decreased markedly from 70 to 3.6 mA in the first 2 h. It was also noticed that the first reduction wave at the tungsten electrode decreased with time and disappeared after 1.8 h of electrolysis. The n-value at this point was found to be 2.73 which was close to the n-value of 2.67 for reducing Ta(V) to the Ta_6^{14+} cluster. The voltammograms showed a significant change. Typical square wave voltammograms at the tungsten electrode after 1.8 h are shown in Fig. 10a. These voltammograms were very similar to those for a $Ta_6Cl_{12}^{2+}$ cluster coating on a glassy carbon electrode in $AlCl_3$-$NaCl_{sat}$ melt (Fig. 10b). At this point the electrolysis current had decreased to 3.6 mA, and the electrolysis became very slow. We also found that the current of the square wave voltammograms at the tungsten electrode for the tantalum cluster gradually decreased (Fig. 10c). The final n-value was observed to be approximately five. When the electrolysis was completed, the waves for the tantalum cluster disappeared, and the melt became almost colorless.

At a higher temperature, 450°C, the n-values were found to be 1, 5, and 5 for the first, second, and third reduction waves, respectively, from the exhaustive electrolyses at −0.5, −0.75, and −1.0 V *vs.* Ag/AgCl. The melt became greenish and finally colorless in the case of the electrolyses at −0.75 and −1.0 V; the glassy carbon electrodes (crucibles) were coated by a shiny metallic film. This shiny film was identified as metallic tantalum by means of x-ray diffraction.

Additional information for the second reduction wave was extracted from the square wave voltammogram of the melt which had been exhaustively electrolyzed at −0.5 V. The forward width was determined to be 60.2 mV, from which the n-value of 2.02 was obtained. This result was in excellent agreement with that given for this reduction wave in Table VI.

Thick black deposits were formed on small Ni or Pt electrodes by controlled-potential electrolyses in the potential

Downloaded on 2016-04-08 to IP 130.203.136.75 address. Redistribution subject to ECS terms of use (see ecsdl.org/site/terms_use) unless CC License in place (see abstract).

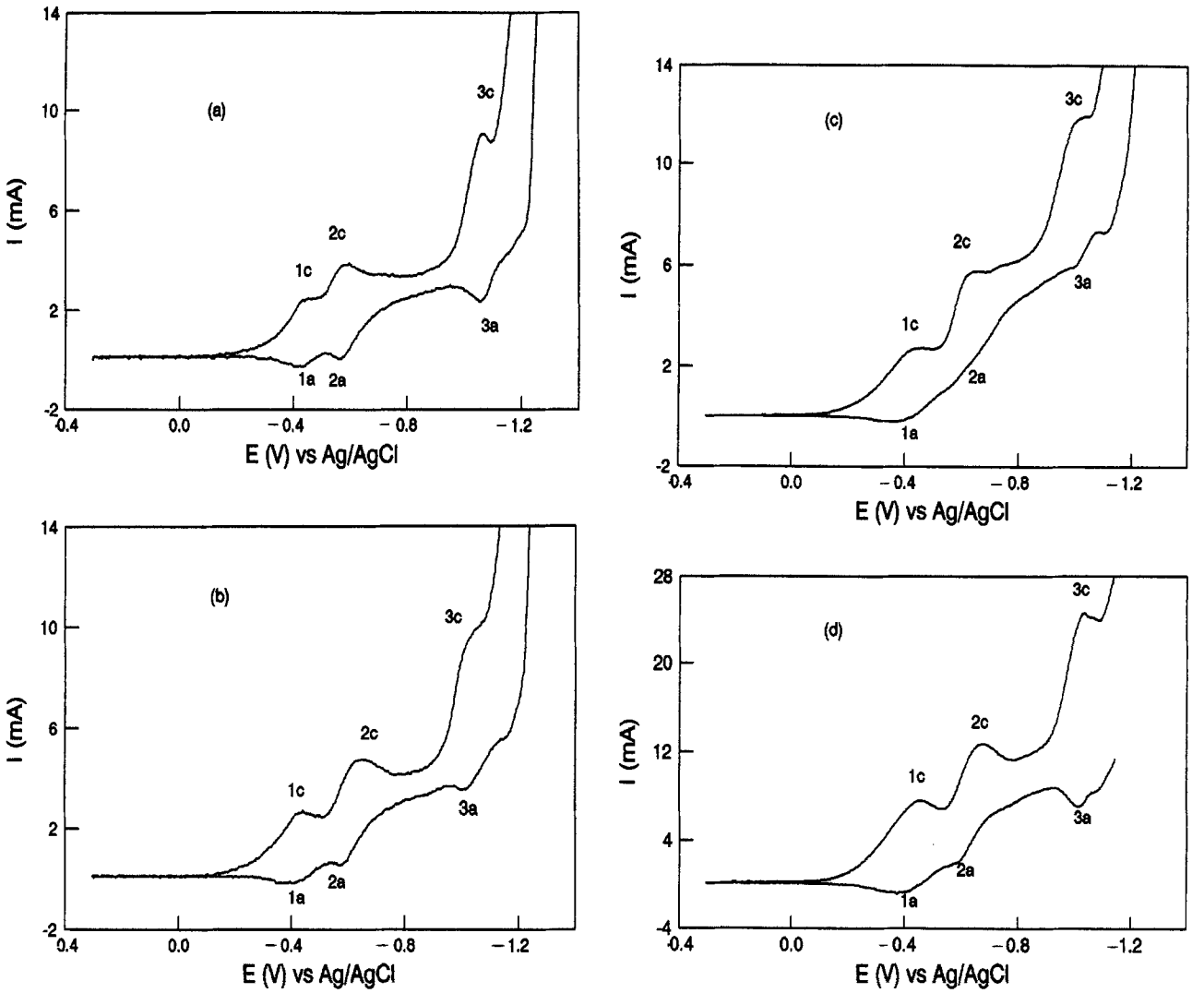

Fig. 9. The forward and reverse current square wave voltammograms of tantalum(V) (37.6 × 10^{-3} mol/kg) in the $NaAlCl_4$-NaF (90-10 m/o) melt. Tungsten electrode: 0.175 cm^2; step potential: 2 mV; pulse amplitude (E_{sw}): 25 mV. (a) 350°C, 10 Hz; (b) 400°C, 10 Hz; (c) 450°C, 10 Hz; (d) 450°C, 100 Hz.

region of the second and third cathodic waves at a temperature of 450°C. The black deposit which was formed in the third cathodic wave region at 200-450°C, was identified by x-ray diffraction to contain a tantalum cluster (Ta_6Cl_{14}) mixed with the melt. Green aqueous and ethanol solutions were obtained by dissolving this black deposit in distilled water in air and in ethanol under an inert nitrogen atmosphere. Both of these solutions gave the same UV-visible spectrum. Several well-defined absorption maxima were observed at 282, 330, 398, 470, 638, and 748 nm. These data were in excellent agreement with Kahn and McCarley's[2] and our previous results[5] for $Ta_6Cl_{12}^{2+}$ in aqueous solution, indicating that the black deposit formed at the potential region of the third wave contained the $Ta_6Cl_{12}^{2+}$ cluster.

Table VII. Exhaustive electrolysis data for Ta(V) in the $NaAlCl_4$-NaF (90-10 m/o) melt.

Temperature (°C)	E(V) *vs.* Ag/AgCl	n-value
210	−0.75 (wave 1c)	2.05
205	−1.0 (wave 3c)	2.73,[a] 5.07[b]
450	−0.5 (wave 1c)	0.98
450	−0.75 (wave 2c)	4.95
450	−1.0 (wave 3c)	4.98

[a] This n-value corresponds to the time when no reduction wave of Ta(V) could be observed in the cyclic and square wave voltammograms at a Pt electrode in the same cell.
[b] This n-value was the final value when no waves for the $Ta_6Cl_{12}^{2+}$ cluster from square wave voltammograms were observed.

A black deposit was also formed on small electrodes at the potential region of the second reduction wave at 450°C. When this black deposit was dissolved in ethanol under a nitrogen atmosphere, a greenish yellow solution was produced. These spectra were quite different from that for a $Ta_6Cl_{12}^{2+}$ solution. Several well-defined absorption maxima were obtained at 238, 282, 348, 424, 640, 760, and 826 nm. The main absorption bands were in very good agreement with the results of McCarley *et al.*[2,3] for $Ta_6Cl_{12}^{3+}$ in ethanol: 235, 274, 344, 431, 735, and 826 nm. The small absorption maximum of 640 nm may indicate that the greenish yellow solution also contained a small concentration of $Ta_6Cl_{12}^{2+}$. Therefore, we may conclude that the black deposit formed at the potentials of the second cathodic wave consisted primarily of $Ta_6Cl_{12}^{3+}$ cluster species.

Thin metallic tantalum deposits were also found using ESCA on the surfaces of the small electrodes which were obtained in the potential region of waves 2 and 3 after dissolving the thick black deposits.

Discussion

Based on the results obtained in this work, it appears that the electrochemical reduction of tantalum(V) in fluorochloroaluminate melts is critically dependent on temperature and is complicated by following chemical reactions.

Waves 1, 1c, and 2, 2c.—As seen above, the first and second reduction waves, which are observed at a higher temperature, merge into one reduction wave at lower tempera-

Downloaded on 2016-04-08 to IP 130.203.136.75 address. Redistribution subject to ECS terms of use (see ecsdl.org/site/terms_use) unless CC License in place (see abstract).

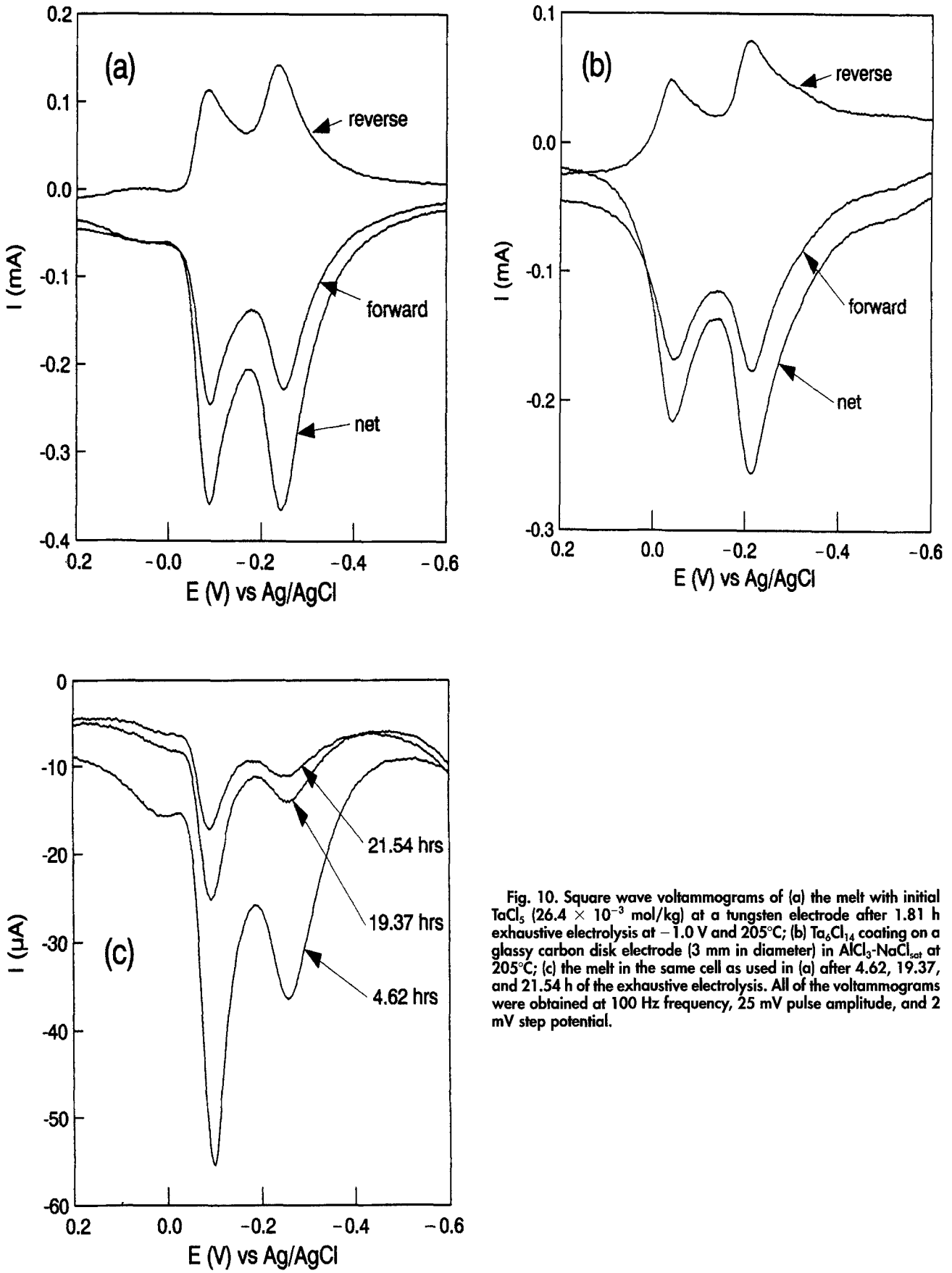

Fig. 10. Square wave voltammograms of (a) the melt with initial $TaCl_5$ (26.4×10^{-3} mol/kg) at a tungsten electrode after 1.81 h exhaustive electrolysis at −1.0 V and 205°C; (b) Ta_6Cl_{14} coating on a glassy carbon disk electrode (3 mm in diameter) in $AlCl_3$-$NaCl_{sat}$ at 205°C; (c) the melt in the same cell as used in (a) after 4.62, 19.37, and 21.54 h of the exhaustive electrolysis. All of the voltammograms were obtained at 100 Hz frequency, 25 mV pulse amplitude, and 2 mV step potential.

tures. Therefore, we discuss these two waves in the same section.

The first reduction wave of tantalum(V) was reasonably well defined in the temperature range 200-450°C, regardless of the voltammetric method. The n-value involved in this reduction wave was determined to be one for the voltammetric time scale at 200-450°C from normal pulse voltammetry (Table V) and square wave voltammetry (Table VI). Also, $n = 1$ was observed for a relatively long time scale at a higher temperature (450°C) based on exhaustive electrolysis (Table VII). Therefore, we conclude that the electron transfer reaction involved in this wave is

Downloaded on 2016-04-08 to IP 130.203.136.75 address. Redistribution subject to ECS terms of use (see ecsdl.org/site/terms_use) unless CC License in place (see abstract).

the reduction of a Ta^{5+} species (believed to be $TaCl_6^-$) to a Ta^{4+} species

$$Ta^{5+} + e^- = Ta^{4+} \quad [3]$$

for short time scales at 200-450°C and for long time scales at higher temperatures (>300°C).

The presence of a following chemical reaction is indicated by the shift of the peak potential of wave 1c in the positive direction with increasing tantalum(V) concentration. Additional evidence is provided by normal pulse voltammetry. In the normal pulse voltammograms at temperatures >350°C, the height ratios of wave 2 to wave 1 are close to one (see Table V). However, the n-value for wave 2 is determined to be two from both normal pulse and square wave voltammograms. The limiting current of a normal pulse wave should be proportional to n and the reactant concentration.[40] The above results may indicate that the concentration of the product is only about half that of the reactant. Therefore, the following chemical reaction of Ta^{4+} is probably the dimerization reaction of the product as follows

$$2Ta^{4+} = Ta_2^{8+} \quad [4]$$

which occurs slowly at <300°C.

At temperatures lower than 300°C, the differences of the n-value, one in the voltammetric time scale, while two in a long time scale (exhaustive electrolysis, Table VII), also support the existence of the following chemical reaction.

Wave 2 or 2c appeared only as the temperature was increased to 300°C for square wave voltammetry and to 350°C for cyclic and normal pulse voltammetries. The n-value from the slope of the linear relationship of E *vs.* ln $[(I_d - I)/I]$ was found to be two (Table V). Square wave voltammetry also produced an n-value very close to two (Table VI). Based on these results, it is reasonable to suggest that the electron-transfer reaction in the second cathodic wave is a two-electron reduction. A well-defined corresponding oxidation wave (2a) was observed in the square wave voltammograms (Fig. 9) while it was not apparent in the cyclic voltammograms (Fig. 5 and 6). These results indicated that the intermediate product (Ta_2^{6+}) was only stable for a very short time. The trivalent tantalum species was also previously observed to be unstable in the $AlCl_3$-EMIC room temperature melt,[15] and acetonitrile.[14] This wave involved a following chemical reaction, since a large anodic stripping wave (4a) appeared when a delay time was applied at the reversal potential of the second wave (Fig. 6). The presence of a preceding chemical reaction (the dimerization of Ta^{4+}) for the second reduction wave was indicated by the change in the peak height ratios of wave 2 over wave 1 with frequency in the net-current square wave voltammograms; the ratio was greater at 10 Hz than at 100 Hz. These results supported the above assumption about the dimerization reaction of Ta^{4+} (reaction 4). $Ta_6Cl_{12}^{3+}$ cluster species was found in the black deposit from the potential-controlled electrolysis at the potentials of the second wave at 450°C using a small electrode. According to these results, the reaction sequence is proposed to be as follows

$$Ta_2^{8+} + 2e^- = Ta_2^{6+} \quad [5]$$

$$9Ta_2^{6+} = 6Ta^{4+} \text{ (or } 3Ta_2^{8+}) + 2Ta_6^{15+} \quad [6]$$

The trivalent tantalum species (Ta_2^{6+}) became less stable as the temperature was increased as indicated by square wave voltammetry (Fig. 9), *i.e.*, the corresponding anodic wave (2a) was less pronounced with an increase in the temperature and at a lower frequency (10 Hz and 450°C).

The cluster species was slowly reduced to metallic tantalum, since a five-electron transfer was observed (Table VII) and a shiny metallic tantalum film was formed on the glassy carbon crucible (with a large surface area) from exhaustive electrolysis.

At temperatures lower than 300°C the first and the second reduction waves merged together when the temperature was decreased from 450 to 200°C in CV, NPV, and SWV studies. Thus, it is reasonable to propose that the first reduction wave observed at a temperature <300°C is an ECEC process which consists of reactions 3, 4, 5 and 6. In this process, reaction 3 is the main reaction while the occurrence of the remaining reactions is limited due to the slow following reactions 4 and 6. This reaction sequence explains reasonably well the results both from CV, NPV and SWV (short time scale) and the exhaustive electrolysis (long time scale). A similar reduction process was previously proposed to explain the electrochemical behavior of Ta(V) in acidic $AlCl_3$-NaCl melts[5] at temperatures <200°C. However, we also notice that the electrochemical behavior of Ta(V) in $AlCl_3$-$NaCl_{sat}$ and $NaAlCl_4$-NaF (90-10 m/o) melts is different from that in acidic melts. By comparing our present and previous results, two well-separated reduction waves are observed in acidic melts[5] while only one reduction wave appears in basic melts at low temperatures. As mentioned in the introduction, the electrochemical behavior of a tantalum chloride species can be examined only after complete removal of the oxide impurities using $COCl_2$ or CCl_4.

A shoulder (wave 1c′) appeared in the cyclic voltammograms at lower temperatures (200 and 250°C) and higher scan rates (Fig. 3 and 4). This shoulder became less significant at lower scan rates or as the tantalum(V) concentration or the temperature was increased. This shoulder may be assigned tentatively to the adsorption of the reduced species according to the theoretical treatments.[41,42]

Wave 3, 3c.—Unlike the second reduction wave which only appeared at temperatures >300 or 350°C, this wave was observed in the whole temperature range studied although the peak height was significantly enhanced as the temperature was increased. The product of the cathodic charge transfer reaction of this wave seemed to be highly unstable since the corresponding oxidation wave (3a) was very small in the cyclic and square wave voltammograms (Fig. 5 and 9). Instead, a large anodic stripping wave composed of waves 4a and 4a′ was observed at much more positive potentials (between 0 and 0.4 V). The n-value involved in wave 3 or 3c′ was approximately equal to two from square wave voltammograms (Table VI). The electron transfer reaction may be written as follows

$$Ta_2^{6+} + 2e^- = Ta_2^{4+} \quad [7]$$

The smaller and ill-defined voltammetric wave at a lower temperature (<300°C) resulted from the limited formation of Ta_2^{6+} species by the slow following chemical reaction (reaction 4).

The product of this step, the divalent tantalum species, decomposes quickly to form the tantalum cluster Ta_6^{14+} (or $Ta_6Cl_{12}^{2+}$) and metallic tantalum, as indicated by the UV-visible spectra of the black deposit dissolved in ethanol or distilled water and the electron spectroscopy for chemical analysis of the electrodeposited electrode surface. The results of exhaustive electrolysis (Fig. 10) also show the formation of the cluster. The following chemical reaction is proposed

$$7Ta_2^{4+} = 2Ta_6^{14+} + 2Ta^0 \quad [8]$$

The exhaustive electrolysis results in the transfer of five electrons (Table VII) and the formation of metallic tantalum film. Figure 10c also shows further reduction of the tantalum cluster. These results indicate that the Ta_6^{14+} cluster is slowly reduced to metallic tantalum.

Waves 4a and 4a′.—From the discussion above, it is obvious that these two anodic stripping waves are associated with the electrochemical oxidation of the tantalum clusters, Ta_6Cl_{15} and Ta_6Cl_{14}, formed in the second and third reduction waves (Fig. 5 and 6).

Acknowledgments

This work was supported by the U.S. Air Force Office of Scientific Research, Grants No. 88-0307 and No. F49620-93-1-0129.

Manuscript submitted Feb. 18, 1993; revised manuscript received May 12, 1993.

Downloaded on 2016-04-08 to IP 130.203.136.75 address. Redistribution subject to ECS terms of use (see ecsdl.org/site/terms_use) unless CC License in place (see abstract).

The University of Tennessee assisted in meeting the publication costs of this article.

REFERENCES

1. R. J. H. Clark and D. Brown, *The Chemistry of Vanadium, Niobium and Tantalum,* Pergamon Press, New York (1973).
2. P. J. Kahn and R. E. McCarley, *Inorg. Chem.,* **4,** 1482 (1965).
3. P. B. Fleming and R. E. McCarley, *ibid.,* **9,** 1347 (1970).
4. J. G. Converse, J. B. Hamilton, and R. E. McCarley, *ibid.,* **9,** 366 (1970).
5. J. H. von Barner, L. E. McCurry, C. A. Jørgensen, N. J. Bjerrum, and G. Mamantov, *ibid.,* **31,** 1034 (1992).
6. T. M. Laher, L. E. McCurry, and G. Mamantov, *Anal. Chem.,* **57,** 500 (1985).
7. G. W. Mellors and S. Senderoff, *This Journal,* **112,** 266 (1965).
8. S. Senderoff, G. W. Mellors, and W. J. Reinhart, *ibid.,* **122,** 840 (1965).
9. S. Senderoff and G. W. Mellors, *Science,* **153,** 1475 (1966).
10. V. I. Konstantinov, E. G. Polyakov, and P. T. Stangrit, *Electrochim. Acta,* **23,** 713 (1978).
11. T. Suzuki, *ibid.,* **15,** 127 (1970).
12. F. Lantelme, A. Barhoun, G. Li, and J. P. Besse, *This Journal,* **139,** 1249 (1992).
13. R. A. Bailey, E. N. Balko, and A. A. Nobile, *J. Inorg. Nucl. Chem.,* **37,** 971 (1975).
14. D. E. Lighter, Jr., J. R. Kirk, and V. Katovic, *J. Coord. Chem.,* **19,** 223 (1988).
15. P. A. Barnard and C. L. Hussey, *This Journal,* **137,** 913 (1990).
16. R. Huglen, F. W. Poulsen, G. Mamantov, and G. M. Begun, *Inorg. Chem.,* **18,** 2551 (1979).
17. L. E. McCurry, Ph.D. Dissertation, University of Tennessee, Knoxville, TN (1978).
18. R. W. Berg, E. Kemnitz, H. A. Hjuler, R. Fehrmann, and N. J. Bjerrum, *Polyhedron,* **4,** 457 (1985).
19. R. G. Kidd and D. R. Truax, *J. Am. Chem. Soc.,* **90,** 6867 (1968).
20. D. E. H. Jones, *J. Chem. Soc., Dalton Trans.,* 567 (1972).
21. B. Gilbert, S. D. Williams, and G. Mamantov, *Inorg. Chem.,* **27,** 2359 (1988).
22. N. Sato, K. D. Sienerth, and G. Mamantov, In preparation.
23. G. Ting, Ph.D. Dissertation, University of Tennessee, Knoxville, TN (1973).
24. I. W. Sun, K. D. Sienerth, and G. Mamantov, *This Journal,* **138,** 2850 (1991).
25. H. Linga, Z. Stojek, and R. A. Osteryoung, *J. Am. Chem. Soc.,* **103,** 3754 (1981).
26. G.-S. Chen, I. W. Sun, K. D. Sienerth, A. G. Edwards, and G. Mamantov, *This Journal,* **140,** 1523 (1993).
27. V. Taranenko, K. D. Sienerth, N. Sato, A. G. Edwards, and G. Mamantov, *Mater. Sci. Forum,* **73-75,** 595 (1991).
28. J. M. Saveant and E. Vianello, *Electrochim. Acta,* **12,** 1545 (1967).
29. C. P. Andrieux, L. Nadjo, and J. M. Saveant, *J. Electroanal. Chem.,* **26,** 147 (1970).
30. J. B. Flanagan, K. Takahashi, and F. C. Anson, *ibid.,* **81,** 261 (1977).
31. Southampton Electrochemistry Group, *Instrumental Methods in Electrochemistry,* p. 220, Ellis Horwood Limited, Chichester (1985).
32. L. Ramaley and M. S. Krause, Jr., *Anal. Chem.,* **41,** 1362 (1969).
33. M. S. Krause, Jr., and L. Ramaley, *ibid.,* **41,** 1365 (1969).
34. J. G. Osteryoung and R. A. Osteryoung, *ibid.,* **57,** 101A (1985).
35. J. H. Christie, J. A. Turner, and R. A. Osteryoung, *ibid.,* **49,** 1899 (1977).
36. J. A. Turner, J. H. Christie, M. Vukovic, and R. A. Osteryoung, *ibid.,* **49,** 1904 (1977).
37. J. J. O'Dea, J. G. Osteryoung, and R. A. Osteryoung, *ibid.,* **53,** 695 (1981).
38. J. Zeng and R. A. Osteryoung, *ibid.,* **58,** 2766 (1986).
39. D. L. Manning and G. Mamantov, *Electrochim. Acta,* **19,** 177 (1974).
40. A. J. Bard and L. R. Faulkner, *Electrochemical Methods,* John Wiley & Sons, Inc., New York (1980).
41. R. H. Wopschall and I. Shain, *Anal. Chem.,* **39,** 1514 (1967).
42. M. H. Hulbert and I. Shain, *ibid.,* **42,** 162 (1970).

Downloaded on 2016-04-08 to IP 130.203.136.75 address. Redistribution subject to ECS terms of use (see ecsdl.org/site/terms_use) unless CC License in place (see abstract).